Sustainable Structures
ISSN: 2789-3111 (Print); ISSN: 2789-312X (Online)
http://www.sustain-dpl.com/journal/sust
DOI: 10.54113/j.sust.2024.000055

ORIGINAL ARTICLE

Mechanical response of glass/kevlar hybrid composite jackets for steel containers carrying hazardous materials to enhance safety

Andrew Kenney, Chao Zhang, Lekhnath Bhandari, Ruifeng Liang, Hota GangaRao *

NSF I/UCRC for Integration of Composites into Infrastructure and Constructed Facilities Center,
West Virginia University, Morgantown, WV, USA
*Corresponding Author: Hota GangaRao, Email: hota.gangarao@mail.wvu.edu.

Abstract: Fiber reinforced (FRP) composite materials have high strength-to-weight ratios and excellent corrosion resistance. Cost reduction manufacturing through methods like Vacuum Assisted Resin Transfer Molding (VARTM) is impressive. This paper deals with composite materials reinforcement of railway tank cars via VARTM to enhance safety, improve fuel efficiency, and reduce adverse environmental impact during derailments aligning with industry goals for safer, sustainable solutions in relation to new railway tank car safety standards. This study investigates different performance aspects of various fiber/fabric configurations (glass, aramid) used as reinforcement with vinyl ester or epoxy. Additionally, core materials like polyurethane and polypropylene have been researched to enhance energy absorption. Effects of through-thickness stitching on mechanical integrity are evaluated for improved puncture resistance. Testing revealed that Kevlar fibers increased energy absorption by increasing strain to failure. Epoxy resin lowered maximum tensile strength by 22% compared to vinyl ester and increased the total energy absorption by 8%. Through-thickness stitching (z-direction) increased tensile strength by 13% and improved interlaminar shear strength.

Keywords: Polymer composite jackets; tank car; vacuum infusion; glass; aramid; core material

1 Introduction

Composite materials have become increasingly prevalent in both the consumer products and industrial applications in recent years[1]. Higher specific strength-to-weight ratio, enhanced toughness and fatigue performance, and excellent corrosion resistance over steel are favorable properties that make composites ideal for the civil, aerospace, marine, mechanical, and automotive industries[2–5]. Finally, advances in production processes of composite materials have brought about reductions in initial cost[6–8]. One such innovative manufacturing process is Vacuum Assisted Resin Transfer Molding (VARTM)[9]. Since the United States Department of Transportation (USDOT) has been introducing new classifications for rail tank cars for DOT-117 and DOT-117R to improve their safety using conventional and expensive steel jacketing techniques[10,11], the authors of this study propose an FRP composite jacketing method to reduce cost and improve energy absorption and puncture resistance using glass/Kevlar hybrid reinforced composites layers as shown in Fig. 1.

This newly proposed FRP composite jacket design embodies many innovative features to improve energy absorption and puncture resistance. The proposed composite jacket can be installed directly over an existing steel tank car which acts as a substrate and negates any use of complicated installation

Received: 25 July 2024; Received in revised form: 14 September 2024; Accepted: 8 October 2024

equipment. The proposed vacuum infusion technique is highly effective, requiring only three days to install a composite tank car. The proposed method is highly cost-effective, and time-saving compared to the traditional methods that involve thermal insulation layers, steel casing, and high temperature welding. The proposed lightweight composite contributes to improved fuel efficiency for tank cars when compared to adding an extra steel layer over existing steel tank cars. By reducing the overall weight of the protective jacket by more than 50% in relation to steel, the design increases load capacity and reduces fuel consumption. This makes the proposed jacket design cost-effective and environmentally friendly to install and operate. These technical aspects are highlighted in this study.

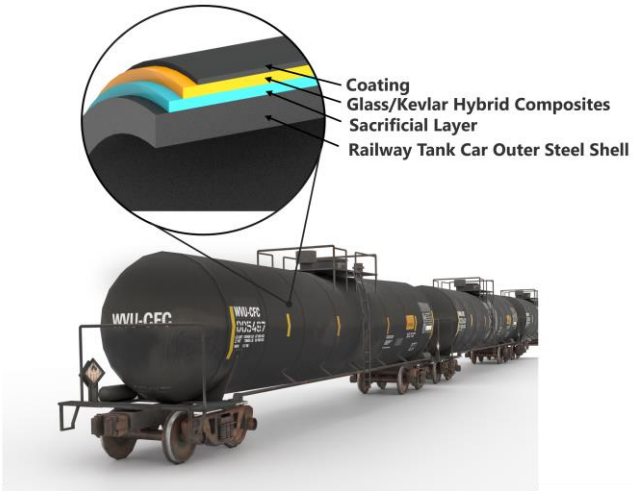

Fig. 1. Proposed FRP composite jacketing for railway tank car.

Composite materials are created by mixing reinforcement fibers and polymeric binders. The type of reinforcements (glass, aramid, Kevlar from Dupont, or carbon) is predefined by the application's needed mechanical properties[12]. Glass fibers are used most widely because of their economy. Aramid fibers have the best puncture and tensile strength, providing them with the best performance properties[13]; however, they are more expensive than glass. The glass/Kevlar hybrid composite jackets offer a unique combination of properties that enhance the overall durability and functionality of the jacket. The glass fibers provide the necessary stiffness, ensuring structural bond, while Kevlar fibers contribute superior tensile strength and puncture resistance. Additionally, the glass fibers are easily soaked in resin to the required shape and mold easily during the infusion process. The proposed hybrid design improves the puncture, resistance, and energy absorption of the jacket and simplifies the manufacturing process, offering a practical and effective solution for tank car protection. FRP composite structures have the potential for carbon reduction and performance improvement in relation to traditional materials[14]. Attention needs to be paid to FRP material performance in extreme conditions, such as fire and safety[15]. Another study, a sequel to this study demonstrates the need to carefully consider preload and initial imperfections in the design of fire-resistant structures using CFRP reinforcements[16].

The choice of resin and its applications is critical to attaining high performance of a composite. Vinyl ester and epoxy are preferred for resin due to their corrosion resistance and other environmental issues. Polyester resin is cheaper and easier to cure resin than others, but it is generally not suitable for structural purposes due to poor tensile strength and chemical resistance[17]. Vinyl ester enhances the properties of polyester resins with chemical resistance and bonding but has poor bonding with fiber[18]. Epoxy, though brittle, is considered to have the strongest molecular bonds, and better quality composite can be made from epoxy in the presence of aramid fibers [19].

Through-thickness (z-direction) stitching is a technology that has been observed to enhance the mechanical integrity of composites. While that might result in some fiber disruption, specific stitching largely enhances interlaminar shear properties and restrains delamination. Thereby reducing early in-plane shear failure and enhances sandwich performance (energy absorption of debonding) [20]. Research by Gnaba et al.[21] have revealed improvements in tensile strength and impact toughness from such a process. Typical core materials include polyurethane and polypropylene, which are fire-

retardant materials[22,23]. Syntactic foams are being used to attain better thermo-mechanical properties[24]. However, railway tank jacketing requires high energy absorption per unit volume, necessitating further research in this area, which this study has undertaken.

While many studies have focused only on one configuration of composite materials, there is still a notable gap within the literature on multifunctional material development to study such factors, particularly in regard to railway tank car shield protection. Therefore, this research filled this gap by evaluating the combined effects of multiple material configurations and reinforcement approaches on the mechanical behavior of composite structures. Specifically, this research focuses on the tensile and bending properties of glass fabric composites, Glass/Kevlar hybrid composites, and composites reinforced with through-thickness stitching. Such improvements are expected to contribute to increased structural integrity, durability, and safety of railway tank cars and enhance service life. In summary, the results of this study advance sustainable material and system designs for railway tank cars, an overarching environmental objective while upholding stringent safety criteria.

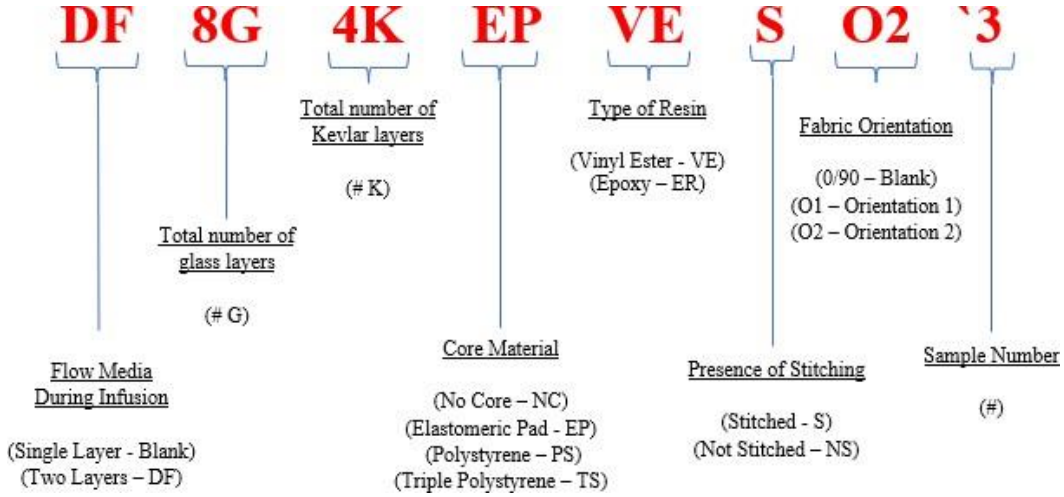

Fig. 2. Specimen naming convention diagram.

2 Specimen nomenclature, preparation, and test setup

2.1 Samples nomenclature

Table 1. Sample nomenclature and descriptions

Test	Specimen Name	Flow Media	Layers	Core	Resin	Stitching
Tension	12GNCVENS	Single layer	12 Glass	NO	Vinyl Ester	Unstitched
	8G4KNCVENS	Single layer	8 Glass & 4 Kevlar	NO	Vinyl Ester	Unstitched
	8G4KNCERNS	Single layer	8 Glass & 4 Kevlar	NO	Epoxy	Unstitched
	8G4KNCVES	Single layer	8 Glass & 4 Kevlar	NO	Vinyl Ester	Stitched
	8G4KPSVENS	Single layer	8 Glass & 4 Kevlar	Polystyrene	Vinyl Ester	Unstitched
Bending	DF8G4KEPVENS	Double layers	8 Glass & 4 Kevlar	Elastomeric Pad	Vinyl Ester	Unstitched
	DF8G4KNCVES	Double layers	8 Glass & 4 Kevlar	NO	Vinyl Ester	Stitched
	DF8G4KNCERS	Double layers	8 Glass & 4 Kevlar	NO	Epoxy	Stitched
	DF8G4KPSVENS	Double layers	8 Glass & 4 Kevlar	Polystyrene	Vinyl Ester	Unstitched
	DF8G4KEPVENS	Double layers	8 Glass & 4 Kevlar	Elastomeric Pad	Vinyl Ester	Unstitched

A nomenclature to help clarify the different variables corresponding to each sample, as shown in **Fig. 2** and **Table 1**. Each specimen ID uses a one or two-letter combination to denote the following variables in each sample's composition: flow media status during infusion, number of glass layers, number of Kevlar layers, core material, type of resin, presence of stitching, and fabric orientation. An additional number is added after a tick mark at the end of the ID to specify individual samples composed of the same variables. Due to the lengthy nature of these specimen ID's, the samples are also referred to by their shorter sample test numbers.

2.2 Manufacturing

The materials manufactured for this study are 15" × 15" (0.381 meters × 0.381 meters) bidirectional glass fabric, with a density of 0.231 g/in² (162.41 kg/m²) and 15" × 15" (0.381 meters × 0.381 meters) Kevlar sheets, with a density of 0.116 g/in ²(81.56 kg/m ³). A layer of glass, sealant tape, and plastic peel ply was applied to the top of the glass pane, with the sealant tape creating an airtight seal and sealing putty placed around the perimeter.

The stitching method involved a 1-inch (2.54 cm) spacing of stitching rows, each containing eight stitches per inch. These samples were through-thickness stitched using an industrial Dürkopp Adler 204-370 sewing machine. The samples were stitched using 2 and 4 denier aramid threads for the bobbin and spool. The use of 8 Glass 4 Kevlar in samples stems from a particular layering pattern: 1 layer of glass fabric, 1 layer of Kevlar fabric, and then another layer of Glass fabric, followed through the composite. This was done to eliminate Kevlar's weakness in resin impregnation and interlayer strength. By putting Glass fabric next to Kevlar, the cohesive strength of the composite can be increased.

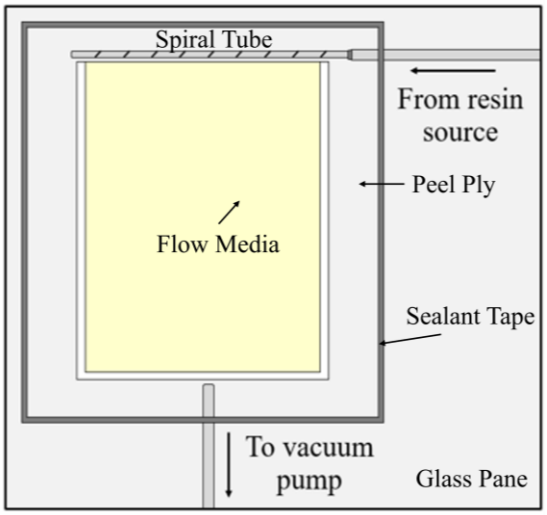

Fig. 3. A diagram illustration of VARTM.

The resin inlet and vacuum outlet tubing were set up with a spiral cut tube for even resin flow, flow media to enhance infusion speed, and a resin catch pot for vacuum pump protection, with peel ply placed around the perimeter; two resin systems, vinyl ester Stypol 040-8086 and Sikadur Hex300, were studied. The vacuum level was monitored by a pressure gauge attached to the vacuum pump and set up to 28 inHg (711 Torr). The viscosity of the resin at injection would be approximately 300 cp ~500 cp to allow it to flow and impregnate the reinforcement material well. When dispensing the resin into the mold, the temperature was set at 25 ℃, and this was also maintained for the mold to ensure uniform distribution of the resin and to prevent its early curing. Gel time is the duration before the resin starts to harden. Then, to complement the main curing, which lasted from 3 to 24 hours, post-curing at a higher temperature of 75 ℃ was continued for an additional 2-12 hours to improve the mechanical properties of the final composite material. The fibre volume fraction in the composites was determined using the burn test, and for glass fabric, the measurement was 55%. Because of problems with Kevlar fabric in this study, its volume fraction was excluded from the calculations. More details can be found in the author's previous work [25].

2.3 Test Setup

Initial tension testing followed ASTM D3039/D3039M[26] for tensile properties, as represented in **Fig. 4** (a). The samples were prepared by cutting from VARTM process, applying steel grip tabs (1" x 3" x 1/8", with drilled holes for better adhesive contact) to prevent slipping, and attaching them with Pliogrip adhesive as shown in **Fig. 4** (b). After a 24-hour cure and excess adhesive sanded off, samples were placed in an Instron 8501 hydraulic testing machine that applied increasing tension recorded at 10 Hz to the sample until failure. Sample dimensions were typically 14.5 inches (36.8 cm) by 1 inch (2.54 cm), with variable thicknesses of 0.15 to 0.2 inches (0.381 to 0.508 cm), trimmed to remove potentially void-rich areas near the infusion inlet and outlet. Three-point bending tests were conducted in accordance with ASTM D7264/D7264M (**Fig. 4** (c))[27]. A three-point bend fixture places the test samples on two supports; the applied force is central. Sample preparation for the bending tests used the same steps as those for tension tests. A constant support span of 10 cm was maintained for all tests to ensure appropriate span-to-thickness ratios, usually ranging between 16:1 and 20:1 according to the sample thickness. The mechanical testing of composite samples was conducted under a displacement control mode with a loading speed of 0.05 inches (1.27 mm) per minute. The data acquisition system continuously records the position and force of the grips with a frequency of 10 Hz.

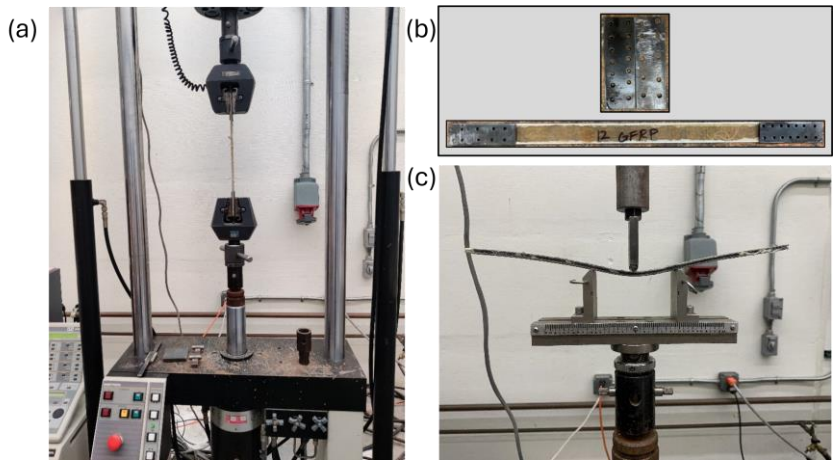

Fig. 4. (a) Tension test, (b) Metal tabs strengthening sample ends, and (c) Bending test.

3 Results and discussion

This section discusses test results of coupons that were subjected to tension and bending. The discussion is based on strain data collated by placing SR-4 strain gages and a universal test machine. The discussion focuses on samples made of glass/Kevlar composites.

3.1 Tension Response

3.1.1 Verification of Instron Machine Strain Data Using Strain Gages

From the test data, several mechanical properties of each sample are calculated. The maximum tensile strength of each sample was obtained directly from the machine by taking the maximum tensile force and dividing it by the average of the measured area of each sample at three different locations. From the literature review[28], it is established that these tensile values, including energy absorption information, provide a good sense of the overall mechanical strength of each sample. **Fig. 5** shows the stress vs. strain values for 12-layer glass fiber fabric with vinyl ester resin, no core material, and no stitching. Samples 12GNCVENS'1, 12GNCVENS'2, 12GNCVENS'3, and 12GNCVENS'4 exhibited a linear response to 90% of the failure strain. Although some variations are observed in 12GNCVENS'1, which slightly lowers the modulus, it is still considered to be within the linear range.

The strains found in **Fig. 5** were based on crosshead displacement of the machine grips and did not directly measure the strain. This method provides a reasonable approximation, but sample slip from the grips (kinks) can lead only to approximate strains. Therefore, the accuracy of machine-based strains is verified with the strain data obtained from strain gauge readings. The adjusted strain data from the slip at the grip location is shown in **Fig. 6**.

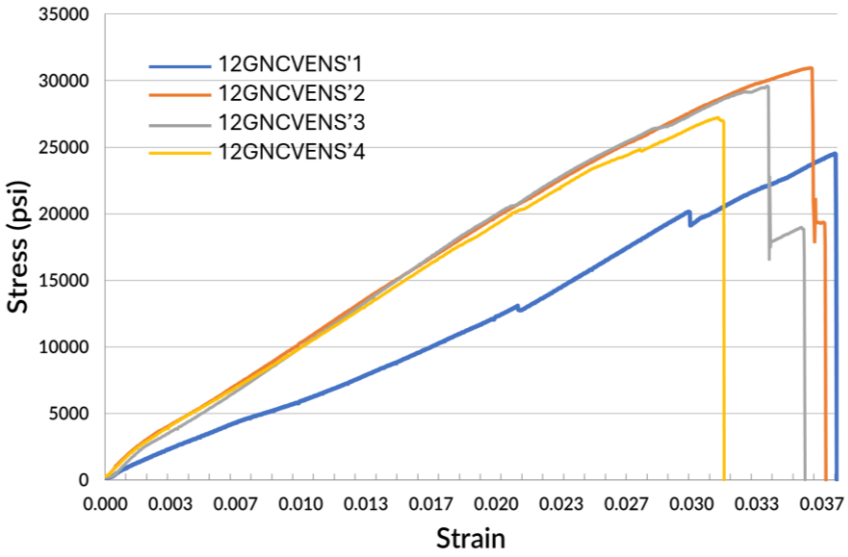

Fig. 5. Stress-Strain curves of samples 12GNCVENS.

The two strain values match closely, except for the initial strain below 0.005, which is attributed to the initial slip of test specimens in grips before grips fully engage with test specimens. The drop in strength after the initial drop in strength (~15 ksi (103 Mpa)) is due to partial delamination in the outer layers (**Fig. 6**). Two additional tests were performed to replicate the stress-strain behavior. The average tensile modulus of elasticity is 5.76×10^5 psi (3.967 GPa) based on the machine and 5.62×10^5 psi (3.873 GPa9 based on the strain gauge; the difference between them is 2.5%.

The tensile elastic modulus is calculated by finding the slope of the initial elongation of each sample. The average of sample 12GNCVENS has a tensile strength at failure of 28,074.5 psi (193.5 MPa), a tensile elastic modulus of 895,000 psi (6.18 GPa), an energy absorption of 553.2 in.lb. (62.99 J), and an energy per unit thickness of 2,950.5 in.lb./in. (518.76 J/m).

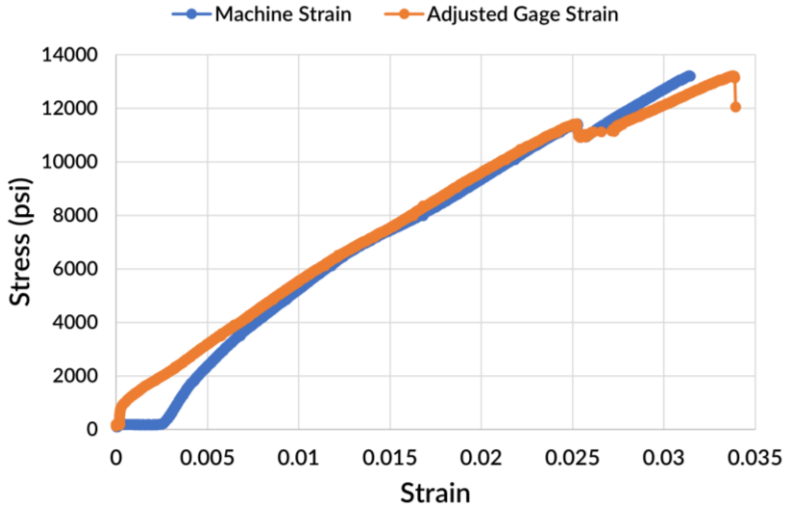

Fig. 6. Machine and adjusted strain vs stress curve

Fig. 7. Failure modes of glass composite under tension

Fig. 7 shows typical failure modes of the glass-only composite samples under tension. Sudden failure of multiple layers at once is initiated, usually near the tips of metal tabs shown in **Fig. 7**. The majority of glass layers fail at once in these samples, demonstrating a high level of cohesion between each layer. This layer debonding does not result in a total loss of strength but does prevent the glass layers from resisting the load.

3.1.2 Glass/Kevlar hybrid composites

After establishing the mechanical properties from 12GNCVENS for all glass samples, Kevlar fabric was introduced to evaluate changes in properties of hybrid (glass+kevlar) composites. The samples in 8G4KNCVENS were made using eight layers of glass fibers and four layers of Kevlar arranged in the standard configuration described in the manufacturing section. These samples are not stitched in the thickness direction and contain no core material, as shown in **Fig. 8**.

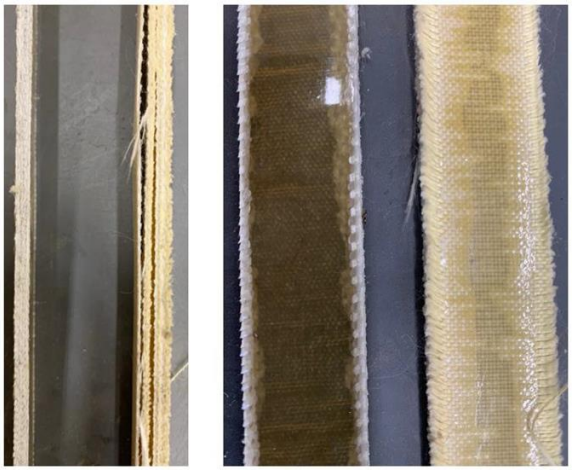

Fig. 8. Comparison between samples 12GNCVENS and 8G4KNCVENS under tension.

When these samples were tested under tension, a significant amount of interlaminar shearing was induced around the edges. During the process of applying tabs and curing, several of the samples began to delaminate before testing. This highlights the importance of keeping a high level of interlaminar shear strength, not only for mechanical strength retention. The mechanical properties of the tested samples are presented in **Fig. 9**.

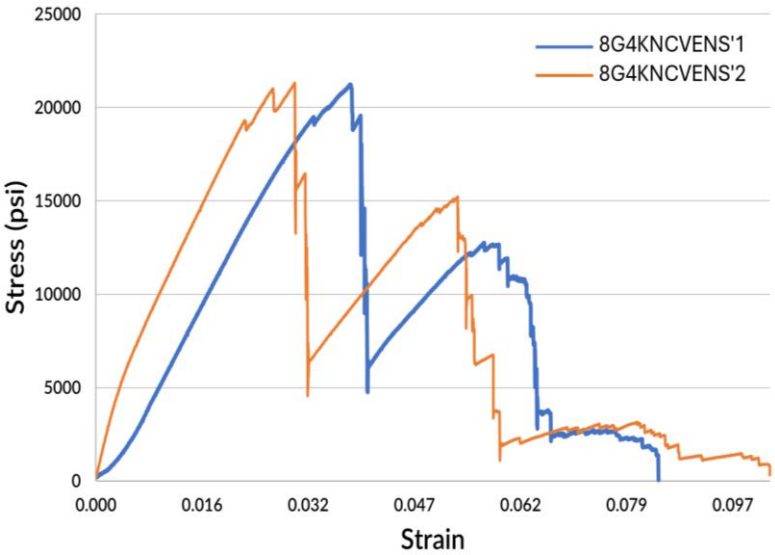

Fig. 9. Stress vs. strain curves under tension of sample 8G4KNCVENS

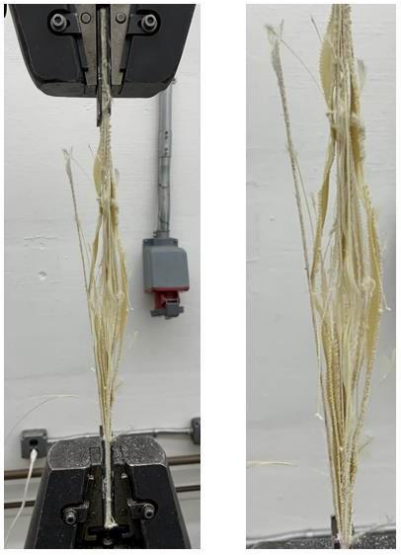

Fig. 10. The failure mode of 8G4KNCVENS samples under tension

The most important distinction between the two samples is the differences in the failure mechanism in **Fig. 9**. The test samples from 12GNCVENS either failed uniformly or underwent a large delamination right before the ultimate failure of the sample. As evident from **Fig. 9**, two distinct peaks are noted. Before the first drop, both the glass and Kevlar layers in the sample acted in unison, distributing the tensile force evenly. However, due to the difference in material stiffness between glass and Kevlar, some layers of the glass fabric failed before the Kevlar, resulting in a huge loss of strength. The load is then transferred to the remaining Kevlar and glass fibers as the amount of stress in the sample begins to increase again. However, due to delamination caused by the initial failure, the amount of remaining interlaminar shear strength in the sample is significantly reduced. The individual Kevlar

layers in the composite, which were partially held in place by the surrounding glass fibers, began to slip and separate from the machine grips, resulting in a further loss of strength at a higher strain rate. This process repeats itself as more glass layers debond and fail, eventually losing all the tensile strength.

The debond Kevlar layer is also evident from the failed specimen, as in **Fig. 10**. This method of failure, where the (layers of a test sample fail first through debond), leading the fibre breakage leads to a rapid decadency in strength, which results in a significant amount of energy absorption before the sample snaps into two parts. The maximum tensile strength (15,891 psi (109.5 MPa)) of these samples is less than those of 12GNCVENS (28,074 psi (194.05 MPa)) due to the fiber layers in 12GNCVENS acting in unison, whereas 8G4KNCVENS had a 43% higher energy absorption and more favorable failure mode, demonstrating Kevlar's effectiveness with glass layers.

3.1.3 Influence of Epoxy VS Vinyl Ester Resin in Glass/Kevlar hybrid composites

The goal of testing 8G4KNCERNS was also to measure the differences in performance between epoxy and vinyl ester resin. The interlaminar shear of test samples was noticeably less significant during the handling and testing process. The stress vs strain values are plotted in **Fig. 11**.

The samples tested from 8G4KNCERNS performed differently from those in 12GNCVENS. In terms of tensile strength, epoxy resin performed worse than the equivalent vinyl ester samples, as shown by the results from 8G4KNCVENS. The effect of resin change is most evident in the stress vs strain curve, i.e., epoxies are more brittle and have lower strain to failure when compared to vinyl esters. Similar to 12GNCVENS, the failure of the sample is primarily localized around a sudden drop in peak strength (as shown in **Fig. 11**).

However, unlike the performance of all-glass sample composites, samples in 8G4KNCERNS did not lose all the strength suddenly at this failure. After this initial major drop in strength, samples resist load, dropping again when there is delamination or fiber slippage, more akin to 8G4KNCVENS's performance. Both of these changes are due to the increase in bond strength provided by the epoxy resin. By providing a large amount of cohesion between glass and aramid fibers, more layers tend to act in unison in the epoxy samples than in the vinyl ester samples. When fibers begin to break, multiple layers of the composite sample break at the same time, resulting in a similar initial drop to that of 12GNCVENS. However, similar to 8G4KNCVENS, the remaining Kevlar layers still provide strength after this breakage, increasing the average energy absorption by 8.4%, which is larger than that of 8G4KNCVENS. The combination of these two properties led to 8G4KNCERNS having the highest average energy absorption of different combinations and demonstrates the effectiveness of epoxy with reference to hybrid composites with Kevlar.

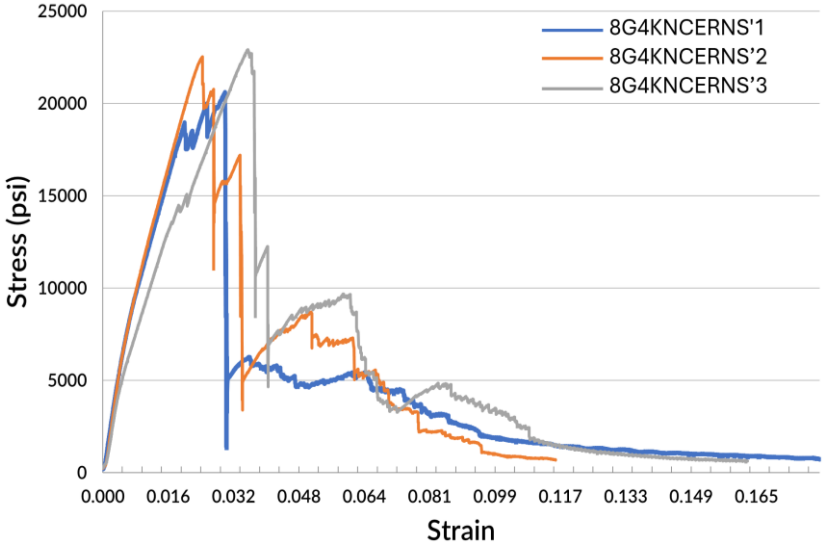

Fig. 11. 8G4KNCERNS (Epoxy Resin) stress vs strain curves under tension.

3.1.4 Stitching effect in Glass/Kevlar hybrid composites

8G4KNCVES was the first test group that used through-thickness stitching to increase the interlaminar shear strength to enhance overall energy absorption. **Fig. 12** shows the fabric stack before and after infusion.

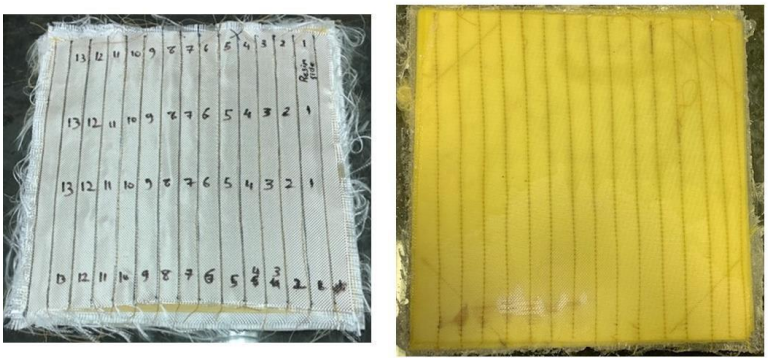

Fig. 12. 8G4KNCVES before and after infusion.

Some areas near the bottom of the fabric stack did not fully infuse, but five test samples with fall infusion were cut and tested for stress-strain response as shown in **Fig. 13**.

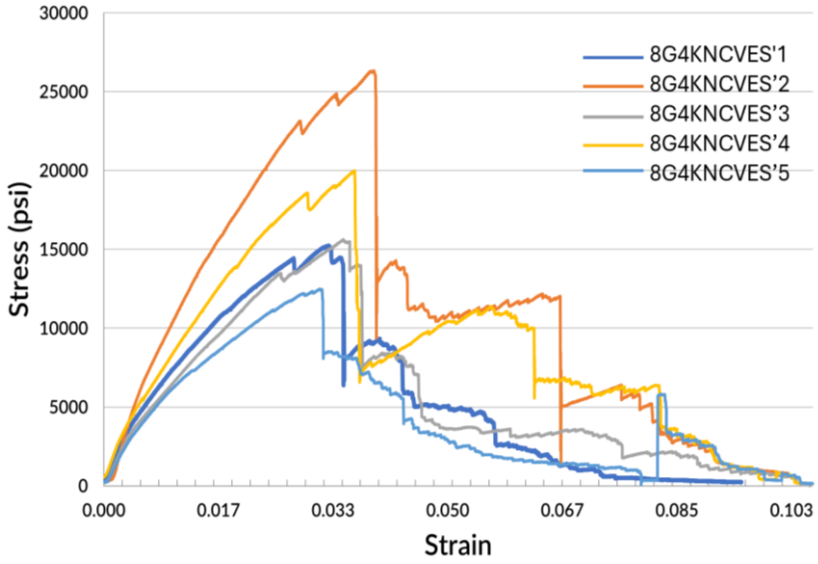

Fig. 13. 8G4KNCVES (Vinyl Ester) stress vs strain curves under tension.

Regarding failure tensile stress resisted by different samples, 8G4KNCVES on average resisted the lowest. However, failure tensile strength of 8G4KNCVES (17,932 psi (123 MPa)) is 12.8% higher than that of 8G4KNCVENS (12,442 psi (86 MPa)). The increased strength of these samples comes from the compaction induced via stitching, which reduced thickness and resulted in a smaller cross-sectional area, increasing the maximum tensile strength of the whole group. The literature review confirms the pre-compaction effect [29], which reduces the amount of entrapped air before the resin is infused. Another notable property change is the 35% reduction in elastic modulus. This, again, is due to through-thickness stitching, as the perforations created during sewing create rows of stress concentrations in the areas around the thread. The stress vs strain curve in **Fig. 13** closely resembles the results from the epoxy-infused samples (8G4KNCERNS). From identify groups, it can be determined that higher levels of shear strength in a composite led to larger initial drops in strength. However, as long as this initial drop is not a final failure of the sample (as seen in 12GNCVENS), the remaining fibers can still resist load, leading to a larger amount of overall energy absorption. The ability of stitching to allow cohesion after failure is also evident when comparing the failed samples to those 8G4KNCVENS after testing (**Fig. 14**). In both sets of images, the sample on the left shows severe delamination but is ultimately held together by the through-thickness stitching. The samples on the right from 8G4KNCVENS show how the lack of cohesion allows each layer to separate completely through

the gripping tabs, leaving the tensile load to be resisted by a few layers or by frictional force resistance, resulting from tightening of the clamps.

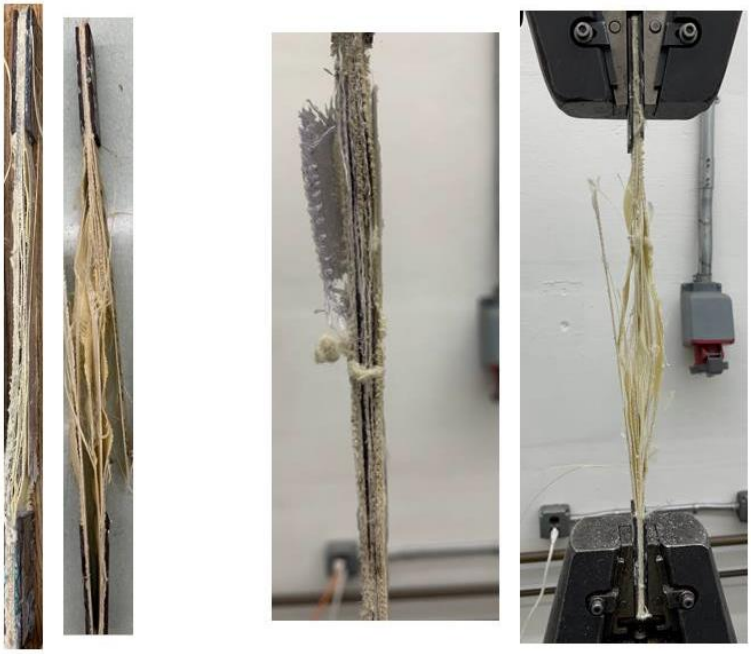

Fig. 14. Comparison of stitched vs non-stitched tested samples.

3.1.5 Sandwich structure using Glass/Kevlar hybrid composites

Two different core materials were tested. The first core is the lightweight, flame-retarding XPS foam. While its mechanical properties are mediocre, the increased thickness from the foam, which only slightly increases the overall weight of the upper layers, allows for greater deformability in the composite. While XPS might decrease tensile strength, it can increase resistance against impact and puncture.

The layup consisted of eight layers of glass, four layers of Kevlar, and one layer of flow media. A 15” x 15” (38.1 cm × 38.1 cm), 0.2” (5.08 mm) thick XPS foam layer was placed at the center such that symmetry was maintained with reference to the core. Various peaks in

Fig. 15 could be attributed to several factors. The two larger peaks are due to the large difference between the tensile stiffness of glass versus Kevlar and smaller peaks corresponding to micro-breakage of fibers with near contribution from the core.

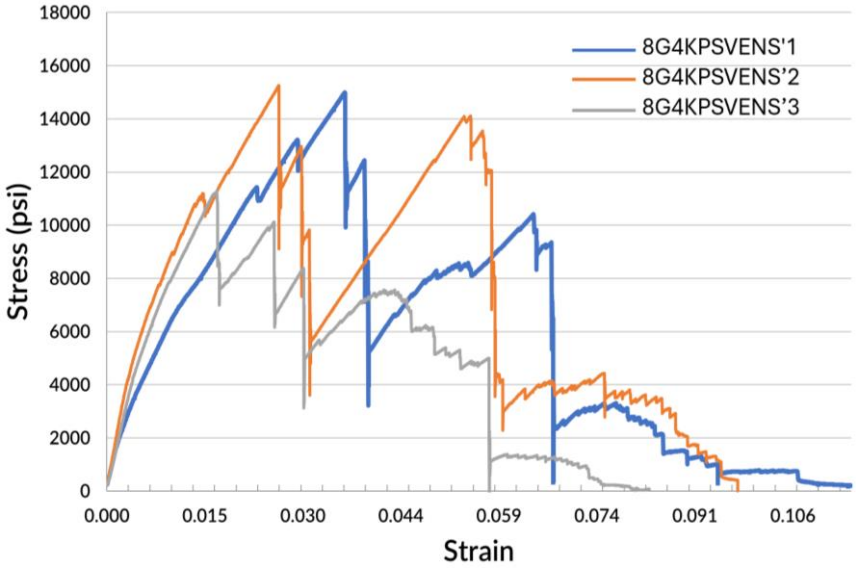

Fig. 15. 8G4KPSVENS (Polystyrene Foam) stress vs. strain curves under tension.

Analysis of the tested samples revealed the influence of XPS core material on mechanical properties, including energy absorption. **Fig. 16** shows that the polystyrene foam had dissolved between its two surrounding layers of glass, leaving the remains bonded to the glass surfaces. The two glass surfaces surrounding one of the foam cores were cut to give a better understanding of the resulting core.

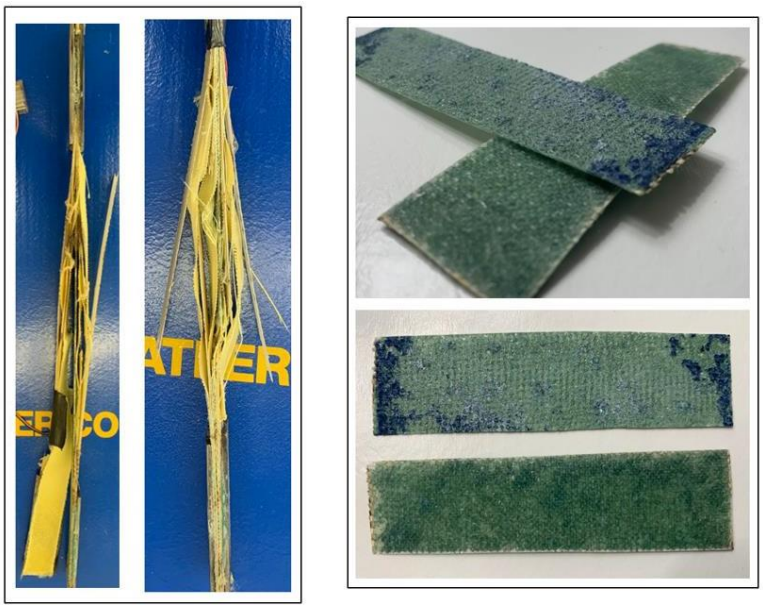

Fig. 16. Failed samples from 8G4KPSVENS (Polystyrene Foam) and removed polystyrene layers.

The 8G4KPSVENS samples had 12.9% lower tensile strength and exhibited the worst mechanical properties compared to 8G4KNCVENS. Total energy absorption and absorption per unit thickness were the lowest among sample-containing Kevlar. These deficiencies in the properties could be attributed to both the insufficient strength of the polystyrene foam and its absorption of resin during the infusion process. The resin absorption by foam, led to a higher void content in the final composite, which most probably weakened the tensile modulus since the stiffness of the composite depends on sufficiently cured resin.DF8G4KEPVENS included an elastomeric pad core in each sample. The elastomeric pad did not shrink or absorb any resin during infusion, so it was decided to use double-flow media.

Fig. 17 shows the stress vs strain curve and mechanical properties for DF8G4KEPVENS.

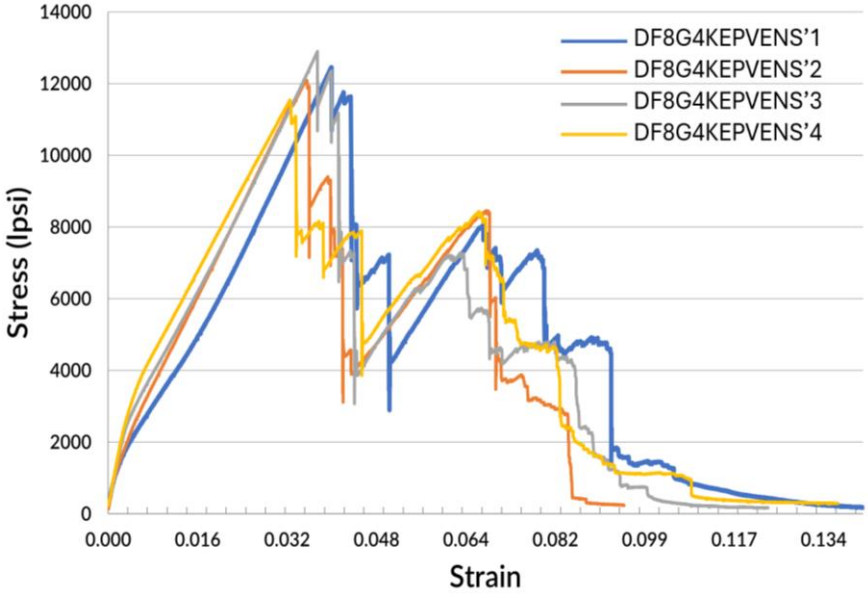

Fig. 17. DF8G4KEPVENS (Elastomeric Pad) stress vs. strain curves under tension.

The resulting mechanical properties from the composite with elastomeric pad were similar to the results of the polystyrene composites, i.e., performance when compared to 8G4KNCVENS having 23% lower tensile strength and 63% lower tensile modulus than the baseline hybrid composite. While this ability to deform is an advantage from an energy absorption viewpoint, it negatively impacts tensile properties.

3.1.6 Tension Tests Summary

Kevlar fabric was added to the glass composite, which improved energy absorption by prolonging the failure mechanism with multiple delamination. The hybrid material configuration, characterized by different stiffnesses and strengths, facilitates the sequential failure of the glass from Kevlar, leading to a more gradual delamination mode. It is noted the glass layers are needed to overcome the inferior resin bond characteristic of Kevlar. Table 2 summarizes the average values for each configuration discussed in this section.

Table 2. Average for Samples with Different Configurations under Tension

Sample ID	Average Tensile Strength at Failure psi (MPa)	Average Tensile Elastic Modulus psi (GPa)	Average Energy Absorption in. lb. (J)	Average Energy per unit Thickness in.lb./in.(J/m)
12GNCVENS	28,074 (193.5)	$8.95x10^5$ (6.18)	553 (62.99)	2,950 (518)
8G4KNCVENS	15,891 (109.5)	$8.30x10^5$ (5.72)	789 (89.31)	4,560 (801)
8G4KNCERNS	12,442 (85.8)	$8.44x10^5$ (5.83)	855 (96.0)	5,524 (971)
8G4KNCVES	17,932 (123.6)	$5.33x10^5$(3.68)	689 (78.56)	4,128 (725)
8G4KPSVENS	13,844 (95.5)	$4.96x10^5$(3.43)	599 (67.99)	2,897 (508.52)
DF8G4KEPVENS	12,242 (84.4)	$3.00x10^5$(2.07)	580 (65.22)	2,234 (392.50)

The use of epoxy resin resulted in a tensile strength reduction of 22% compared with vinyl ester-based samples. The addition of epoxy resin produced an increase in energy absorption by 8% and improved bond resistance of Kevlar with epoxy. Stitching increased the tensile strength by 13% due to the compaction of fabric layers. This can be attributed to the densification of reinforcement, allowing for better load distribution between layers and resulting in increased tensile properties. Besides, stitching resulted in a considerable increase in interlaminar shear strength by delaying delamination due to poor interfacial adhesion between layers.

The presence of an extruded polystyrene foam core had a negative effect on all the mechanical properties, i.e., tensile strength, modulus and energy absorption were lower by 13% and 24%, respectively. While the energy absorbed per unit thickness did decrease by 36%, such losses reveal the addition of foam core weakens the mechanical performance of a composite, making it less suitable for high-load applications; however, thermal and specific weight properties may improve in the presence of suitable foams. This clearly reflects the need for a proper balance between the advantages of weight reduction and thermo-mechanical properties for an application.

The addition of an elastomeric pad as core material showed significant reductions in the mechanical properties, i.e., tensile strength, modulus, and energy absorption were reduced by 23%, 26%, and 51% respectively. The elastomeric pad also added flexibility that was not seen in any other configuration, which can be quantified by measuring the tension strain at the first drop of strength in each sample, which is shown in **Table 3**. Therefore, the strategic placement of the core is intended to optimize displacement response, thereby enhancing energy absorption under impact or puncture [30].

Table 3. Tension strain at first delamination

Tension Strain at First Drop of Strength					
12GNCVENS	8G4KNCVENS	8G4KNCERNS	8G4KNCVES	8G4KPSVENS	DF8G4KEPVENS
0.0381	0.0372	0.0338	0.0379	0.0308	0.0412

3.2 Bending Tests

3.2.1 Glass/Kevlar hybrid composites

Bending tests on DF8G4KNCVES were performed to establish baseline values for comparison. However, this test group incorporated fabric, core, stitching, and reason configuration advantages that were found from the tension tests. The test samples with DF8G4KNCVES configuration are composed of eight glass and four Kevlar layers stitched together at 1" (2.54 cm) spacing because of their optimal response under tension. The maximum flexural strength of the sample was found using equation 1 for rectangular cross-sections with center point load[27].

$$\sigma = \frac{3PL}{2bh^2} \tag{1}$$

Where σ is the peak stress, calculated using the applied force P, the sample's length L, width b, and thickness, this is comparable to finding the maximum tensile strength under bending for each sample. By plotting stress vs strain, the flexural modulus of elasticity is determined. The amount of energy absorption is found by calculating the area under each stress strain curve. The energy values are normalized with a strain-limited energy absorption values which are limited to a strain value 5%.

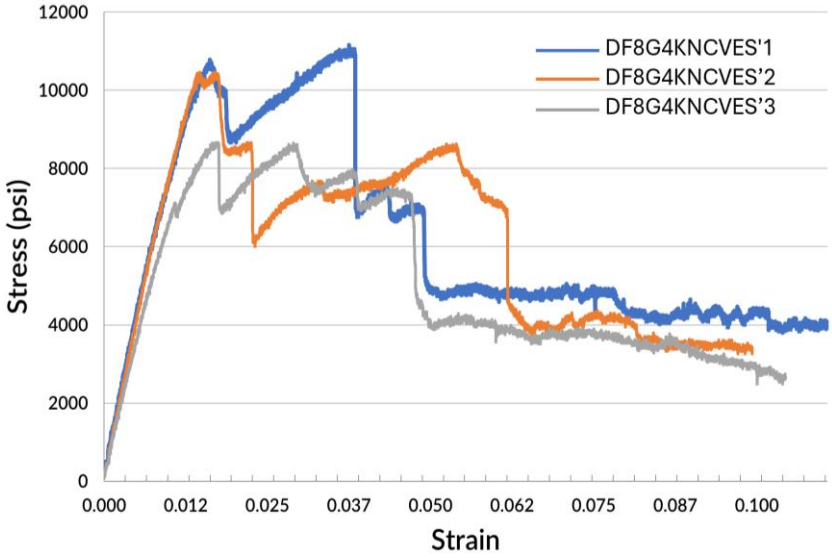

Fig. 18. DF8G4KNCVES (Vinyl Ester) stress vs. strain curves under bending.

All samples demonstrated linear responses to near-peak stress so that the modulus of elasticity with linear zone can be determined within 1% strain as shown in **Fig. 18**. The resistance provided by these composite layers after delamination (~1%) is significantly less than the peak load before delamination. In some test samples (DF8G4KNCVES), multiple layers delaminated at once around 0.04, resulting in a sudden drop in strength.

3.2.2 Resin effect in Glass/Kevlar hybrid composites

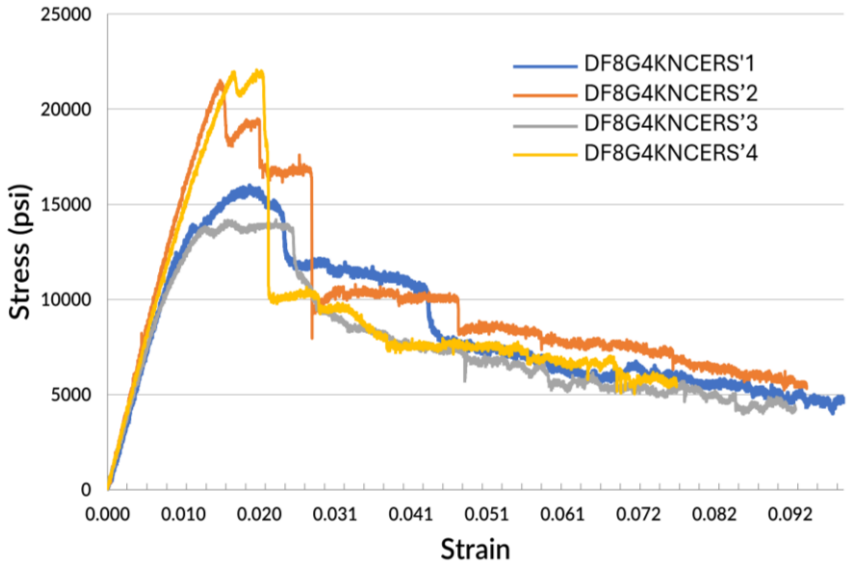

Fig. 19. DF8G4KNCERS (Epoxy Resin) stress vs. strain curves under bending.

DF8G4KNCERS (epoxy) was designed to compare direct strength/stiffness between vinyl ester and epoxy under bending. The samples in this test group are identical to those from DF8G4KNCVES (vinyl ester) except the binder was epoxy resin. The mechanical properties and stress-strain curves of all samples are shown in **Fig. 19**.

While the maximum bending force experienced by epoxy-based samples in DF8G4KNCERS (67.3 lb.) 299.6 N) is comparable to that of vinyl ester-based sample DF8G4KNCVES, the epoxy samples led to an 83% increase in flexural strength. Similar to the differences in the tension tests, the flexural modulus of epoxy samples (18,450 psi (127.2 MPa)) increased by 98% compared to vinyl ester samples (10,099 psi (69.6 MPa)). When comparing the strain-based energy absorption between the two bending test groups, the epoxy samples provided 53% higher energy absorption than the vinyl ester-based samples.

3.2.3 Structure using Glass/Kevlar hybrid composites.

DF8G4KPSVENS uses samples made from the same manufacturing process as DF8G4KNCVES except for the addition of a polystyrene core. DF8G4KPSVENS does not include fabric stitching in its composition. Preliminary tests found that through-thickness stitching of a sample with polystyrene core caused the core to tear before infusion. The thread used during stitching would cut through the polystyrene, leaving large gaps in polystyrene and resulting in test specimen filled with excess resin. Mechanical properties and resulting stress vs. strain curves for DF8G4KPSVENS are shown in 错误! 未找到引用源。.

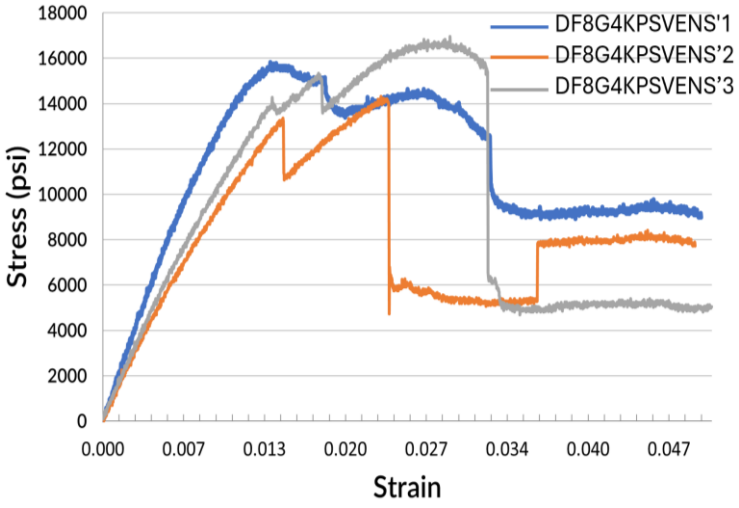

Fig. 20. DF8G4KPSVENS (Polystyrene Foam) stress vs. strain curves under bending

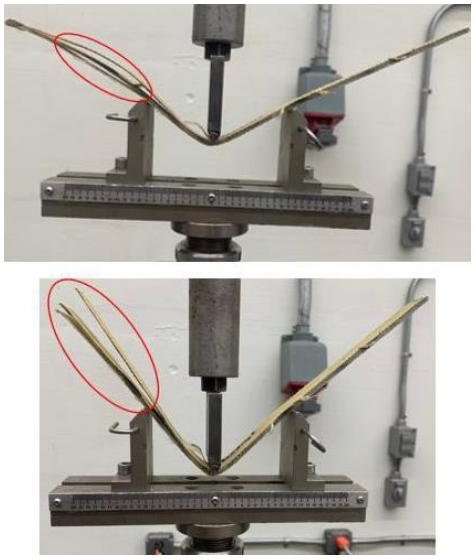

Fig. 21. DF8G4KPSVENS sample delamination under bending

The maximum bending force with polystyrene foam was comparable to that of Groups DF8G4KNCVES and DF8G4KNCERS without foam. The flexural modulus for this sample group was 60% larger than that of DF8G4KNCVES, even though both samples were infused using vinyl ester. This result is due to a stiffened polystyrene core, which again dissolved during the infusion of the sample and bonded to the surrounding glass layers. 错误!未找到引用源。 showcases how the layers suddenly delaminate specifically from these polystyrene glass layers under excessive deformation (l/h ≈ 0.2 to 0.5), resulting in large drops in strength. The strain-based energy absorption of DF8G4KPSVENS went up by 33% when compared to the average of DF8G4KNCVES, which is attributed to stiffened glass fibers with melted polystyrene resin.

The last group was created to study the effect of using an elastomeric pad as a core material. To provide a direct comparison to DF8G4KPSVENS under tension, the normal, unstitched fabric layup was used along with the same thickness for the elastomeric pad. Two layers of flow media were used for the infusion of these samples. The resulting mechanical properties and stress vs strain curves are shown in **Fig. 22**. The elastomeric pad lowered the structural performance of the sample in all measured categories when compared to DF8G4KNCVES, i.e. 89% and 46% decrease in flexural modulus and energy absorption when compared to control sample.

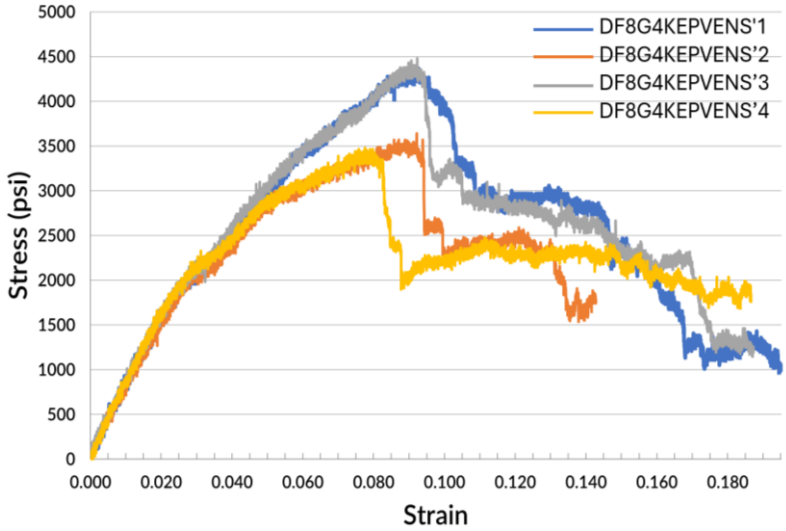

Fig. 22. DF8G4KEPVENS (Elastomeric Pad) stress vs. strain curve under bending.

3.2.4 Bending Tests Summary

The epoxy based composite samples increased in flex strength, modulus and energy absorption by 83% and 53% respectively over vinyl ester infused sample. The use of double flow media in the samples provided an increased infusion speed and prevented formation of large voids on the bottom layers without flow media. However, the practice of using double flow media was discontinued as it does not represent results achievable for the final tank car jacket. **Table 4** summarizes the average values for each configuration under bending discussed in this section.

The use of a polystyrene core increased the average flexural strength modulus and strain-based energy absorption by 55%, 97%, and 33% when compared to a similar sample with no core material. Using an elastomeric pad core decreased the average flexural strength by 60%, flexural modulus by 89%, and strain-based energy absorption by 76% when compared to a similar sample with no core material. A comparison of strains at the first drop of strength (**Table 5**) reveals that the elastomeric pad sample again performs the best.

Table 4. Average for Samples with Different Configurations under Bending

	Max Flexural Strength psi (MPa)	Flexural Elastic Modulus psi (GPa)	Total Energy Absorption in.lb. (J)	Strain-Based Energy Absorption in.lb. (J)	Energy per Unit Thickness in.lb./in. (J/m)
DF8G4KNCVES	10,099 (69.65)	$7.47x10^5$ (5.15)	618.3 (69.92)	356.3 (40.26J)	3,091 (349.61)
DF8G4KNCERS	18,450 (127.22)	$1.48x10^6$ (10.21)	789.9 (89.32)	545.5 (61.64)	4,937 (558.61)
DF8G4KPSVENS	15,694 (108.2)	$1.20x10^6$ (8.28)	550.1 (62.24)	475.4 (53.77)	3,143 (357.89)
DF8G4KEPVENS	3,990.60 (27.52)	$7.91x10^6$ (0.55)	430.4 (48.63)	85.2 (9.63)	1,655 (188.57)

Table 5. Bending strain at first delamination

DF8G4KNCVES	DF8G4KNCERS	DF8G4KPSVENS	DF8G4KEPVENS
0.0203	0.0208	0.0175	0.0940

3.3 Morphology Analysis

Scanning electron microscopy was used to understand the intricate high-volume infusion process in terms of fiber architectures and resin-fabric interaction. The samples (four-glass, eight-Kevlar layer composite infused with vinyl ester resin) were analyzed utilizing SEM to reveal the interplay of resin with fabrics. **Fig. 23** depicted three layers: a thin top layer of resin, a cross-weave pattern of the glass fibers under the top layer, and two thick, uniquely patterned layers of Kevlar.

A deeper examination at 200x to 500x magnification of the Kevlar material found that the smeared look was due to aramid fibers compacted during cuttings, and the corresponding SEM is presented in **Fig. 24**. In comparison, progressing at higher magnification of SEM images, as in **Fig. 25** indicated, made resin in the glass fiber infiltration easier than the Kevlar counterpart[31].

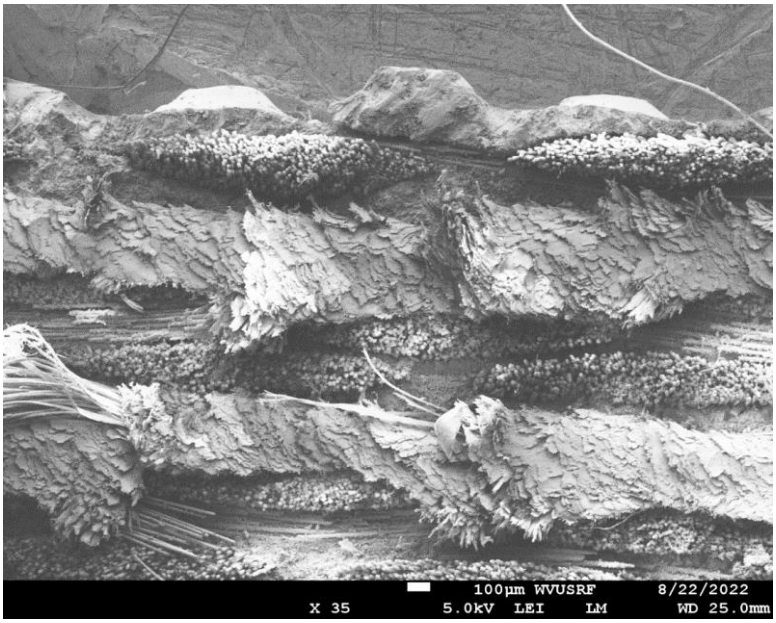

Fig. 23. SEM cross section of the composite 8G4KNCVENS.

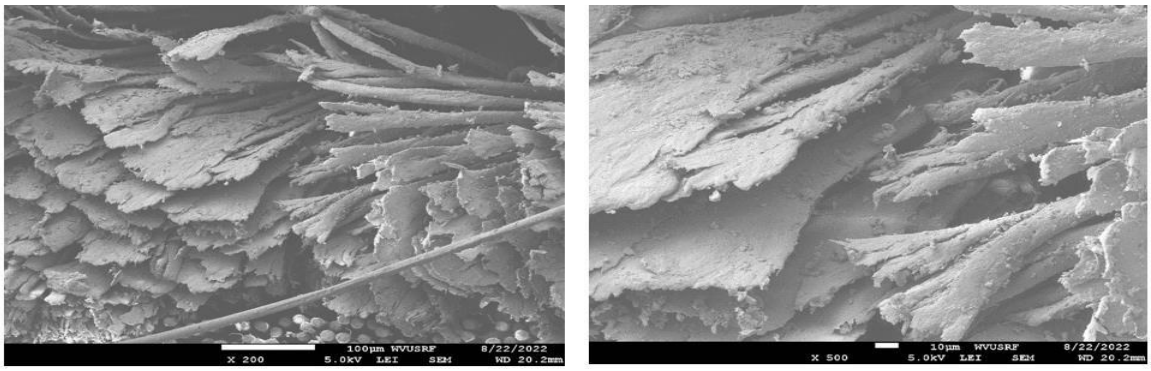

Fig. 24. SEM 200x and 500x magnification images of the Kevlar fibers.

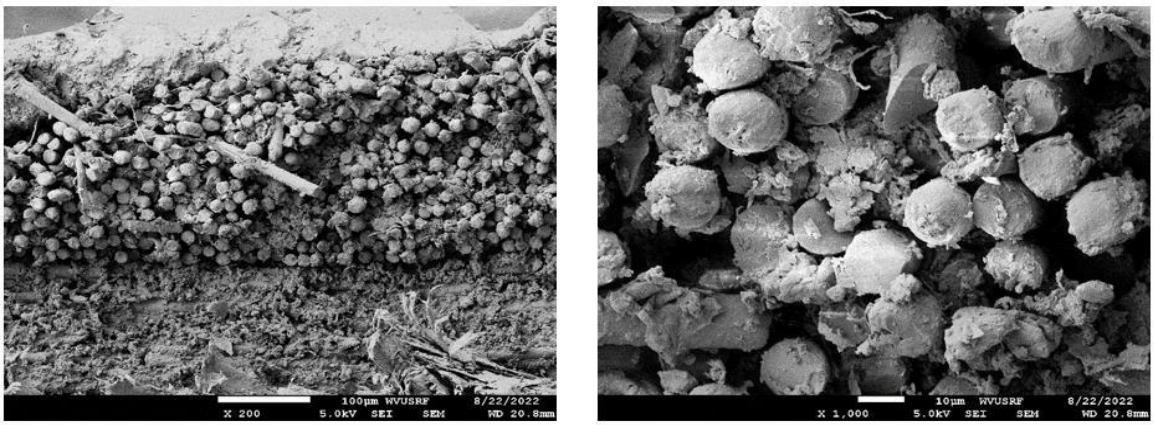

Fig. 25. SEM images of resin permeating the glass fibers for sample 8G4KNCVENS.

4 Conclusions

Axial and bending responses of hybrid composite samples containing Kevlar and glass fabrics with epoxy or vinyl ester resins, and with and without through-thickness (z-direction) stitching, including core materials, are presented herein. Hybrid composites (Kevlar plus glass) recorded higher energy absorption than glass fabric composites. Hybrid composites are cost-effective glass layers and easy to infuse with Kevlar. Epoxy resin increased the energy absorption by 8%, and the modulus of elasticity

was the same in both bending and tension tests. However, tensile strength to failure decreased by 22% when epoxy was used.

Stitching reduced the tensile elastic modulus by 36% and increased the interlaminar shear strength and the tensile strength by 13%. The core material of extruded polystyrene foam reduced the maximum tensile strength by 13% while the bending strength increased slightly. An elastomer pad core reduced the mechanical properties in tension and bending but improved strain to the first drop (reduction) in flexural of strength. SEM results show that glass fiber is easier to bond with resin than Kevlar fiber.

The presence of Kevlar fibers in the composite extended the failure strain beyond the peak stress, with energy absorption remaining significant at lower stress levels (~40% of the peak) when measured up to 5% strain. Epoxy resin improved the energy absorption and modulus of elasticity. However, it lowered the tensile strength by 22%. Stitching enhanced tensile strength and interlaminar shear strength but reduced tensile elastic modulus by 36%.

Practical Implications for the Railway Industry

The results obtained from this study have major practical implications for the railway industry in the development and performance improvement of railway tank cars. A hybrid composite configuration comprising glass and aramid fibers thus offers a balanced approach between cost-effectiveness, high energy absorption, and puncture resistance. Enhanced energy absorption is achieved in the presence of Kevlar fibers. The enhanced interlaminar shear strength and tensile strength from z-directional stitching increased composite strength for better resistance from delamination and puncture. Integrating hybrid composite jackets with steel shells into railway tank cars will yield safer, stronger, and more cost-effective solutions than steel jacketing.

Funding Statement

This research was supported by the U.S. Department of Transportation Pipeline and Hazardous Materials Safety Administration under Contract No. 693JK320C000008, through the NSF Industry-University Collaborative Research Center Membership Program at West Virginia University. Additionally, the Center for Integration of Composites into Infrastructure (CICI) at the NSF IUCRC is funded by the National Science Foundation under Award No. 1916677, which has partially syggested this research.

Acknowledgments

Authors express their appreciation to USDOT-PHMSA for their contributions to this project.

CRediT authorship contribution statement

Andrew Kenney: Investigation, Formal analysis, Writing – original draft. **Chao Zhang**: Investigation, Formal analysis, Writing – original draft **Lekhnath Bhandari**: Testing, Investigation. **Ruifeng Liang**: Supervision, Investigation, Writing – review & editing, **Hota GangaRao:** Conceptualization, Funding acquisition, Supervision, Formal analysis, Investigation.

Conflicts of Interest

The authors declare that they have no conflicts of interest to report regarding the present study.

References

[1] Yao SS, Jin F-L, Rhee KY, Hui D, Park S-J. Recent advances in carbon-fiber-reinforced thermoplastic composites: A review. Compos Part B 2018; 142: 241–50. https://doi.org/10.1016//j.compositesb.2017.12.007.

[2] Sun M, Kumar N, Dhinojwala A, King H. Attractive forces slow contact formation between deformable bodies underwater. Proc Natl Acad Sci 2021; 118;41:e2104975118.https://doi.org/10.1073/pnas. 210497511.

[3] Li F, Gan J, Zhang L, Tan H, Li E, Li B. Enhancing impact resistance of hybrid structures designed with triply periodic minimal surfaces. Compos Sci Technol 2024; 245:110365.https://doi.org/10.1016/j.compscitech.2023.110365.

[4] Banik A, Zhang C, Panyathong D, Tan KT. Effect of equienergetic low-velocity impact on CFRP with surface ice in low temperature arctic conditions. Compos Part B Eng 2022; 236:109850.https://doi.org

/10.1016/j.compositesb.2022.109850.
[5] Liu T, Liu X, Feng P. A comprehensive review on mechanical properties of pultruded FRP composites subjected to long-term environmental effects. Compos Part B Eng 2020; 191:107958.https://doi.org /10.1016/j.compositesb.2020.107958.
[6] Li B, Liu Y, Tan K-T. A novel meta-lattice sandwich structure for dynamic load mitigation. J Sandw Struct Mater 2019; 21;6:1880–905. https://doi.org/10.1177/1099636217727144.
[7] Zhang C, Tan KT. Low-velocity impact response and compression after impact behavior of tubular composite sandwich structures. Compos Part B Eng 2020: 108026.https://doi.org/10.1016/j.compositesb. 2020.108026.
[8] Liang R, Hota G. Development and evaluation of load-bearing fiber reinforced polymer composite panel systems with tongue and groove joints. Sustain Struct 2021; 1;2.https://doi.org/10.54113/j.sust.2021. 000008.
[9] Song X. Vacuum assisted resin transfer molding (VARTM): model development and verification 2003. https://doi.org/hdl.handle.net/10919/27168 Collections.
[10] Rakoczy P, Carolan M, Gorhum T, Eshraghi S. Side Impact Test and Analyses of a DOT-117 Tank Car. United States. Federal Railroad Administration. Office of Research …; 2019.
[11] Hu P, Schmitt R, Fan C-C, McGill J. Fleet Composition of Rail Tank Cars Carrying Flammable Liquids: 2022 Report 2022. https://doi.org/10.21949/1527850.
[12] Morgan PW, Kwolek SL, Pletcher TC. Aromatic azomethine polymers and fibers. Macromolecules 1987; 20;4:729–39. https://doi.org/10.1021/ma00170a006.
[13] Summerscales J, Dissanayake NPJ, Virk AS, Hall W. A review of bast fibres and their composites. Part 1– Fibres as reinforcements. Compos Part A Appl Sci Manuf 2010; 41;10:1329–35.https://doi.org/10.1016/ j.compositesa.2010.06.001.
[14] Liu T, Tang J-T, Zhang S, Dong L, Hu L, Meng X, et al. Carbon emissions of durable FRP composite structures in civil engineering. Eng Struct 2024; 315:118482.https://doi.org/10.1016/j.engstruct.2024. 118482.
[15] Thongchom C, Hu L, Sanit-in PK, Kontoni D-PN, Praphaphankul N, Tiprak K, et al. Experimental Investigation on Post-Fire Mechanical Properties of Glass Fiber-Reinforced Polymer Rebars. Polymers (Basel) 2023; 15;13. https://doi.org/10.3390/polym15132925.
[16] Liang X, Wang W, Hu L, Feng P. Experimental and numerical study on high-temperature performance of prestressed CFRP-reinforced steel columns. Eng Struct 2024; 301:117347.https://doi.org/10.1016/j. engstruct.2023.117347.
[17] Velmurugan R, Solaimurugan S. Improvements in Mode I interlaminar fracture toughness and in-plane mechanical properties of stitched glass/polyester composites. Compos Sci Technol 2007; 67;1:61–9. https://doi.org/10.1016/j.compscitech.2006.03.032.
[18] Jiao W, Liu W, Yang F, Jiang L, Jiao W, Wang R. Improving the interfacial property of carbon fiber/vinyl ester resin composite by grafting modification of sizing agent on carbon fiber surface. J Mater Sci 2017; 52:13812–28. https://doi.org/10.1007/s10853-017-1485-8.
[19] Marouani S, Curtil L, Hamelin P. Ageing of carbon/epoxy and carbon/vinylester composites used in the reinforcement and/or the repair of civil engineering structures. Compos Part B Eng 2012. https://doi.org/10.1016/j.compositesb.2012.01.001.
[20] Song C, Fan W, Liu T, Wang S, Song W, Gao X. A review on three-dimensional stitched composites and their research perspectives. Compos Part A Appl Sci Manuf 2022; 153:106730 https:.//doi.org/ 10.1016/j.compositesa.2021.106730.
[21] Gnaba I, Legrand X, Wang P, Soulat D. Through-the-thickness reinforcement for composite structures: A review. J Ind Text 2019; 49;1:71–96. https://doi.org/10.1177/152808371877229.
[22] Banik A, Zhang C, Khan MH, Wilson M, Tan KT. Low-velocity ice impact response and damage phenomena on steel and CFRP sandwich composite. Int J Impact Eng 2022; 162:104134. https://doi.org/10.1016/j.ijimpeng.2021.104134.
[23] San Ha N, Lu G. A review of recent research on bio-inspired structures and materials for energy absorption applications. Compos Part B Eng 2020; 181:107496. https://doi.org/10.1016/j.compositesb.2019.107496.
[24] Zhang L, Zhang F, Liu M, Hu X. Novel sustainable geopolymer based syntactic foams: An eco-friendly alternative to polymer based syntactic foams. Chem Eng J 2017; 313:74–82.https://doi.org/10.1016/j.cej. 2016.12.046.
[25] Kenney A. Mechanical Response of VARTM infused FRP composites 2022. https://doi.org/10.33915/etd. 11473.
[26] Materials ACD-30 on C. Standard test method for tensile properties of polymer matrix composite materials. ASTM international; 2008. https://doi.org/10.1520/D3039_D3039M-08.
[27] ASTM D. D7264/D7264M-21; Standard Test Method for Flexural Properties of Polymer Matrix Composite Materials. West Conshohocken, Pennsylvania ASTM Int 2021. https://doi.org/10.1520/D7264 _D7264M-21.

[28] Vadlamani D. Strain energy density based failure criterion for GFRP coupons under tension and bending. West Virginia University; 2007. https://doi.org/10.33915/etd.1814.
[29] Hamidi YK, Aktas L, Altan MC. Effect of packing on void morphology in resin transfer molded E-glass/epoxy composites. Polym Compos 2005;26;5:614–27. https://doi.org/10.1002/pc.20132.
[30] Bhandari L. Evaluations of FRP Composite Coupons Under Impact and Puncture. West Virginia University; 2023. https://doi.org/10.33915/etd.12142.
[31] Ramasamy N, Arumugam V, Rajkumar S. Surface modification of Kevlar fibre fabric and its influence on the properties of Kevlar/epoxy composites. Bull Mater Sci 2019; 42:1–9.https://doi.org/10.1007/s12034 - 019-1868-3.